An Overloaded IoT Signal Detection Method using Non-convex Sparse Regularizers

Kazunori Hayashi*, Ayano Nakai-Kasai†, Atsuya Hirayama,‡ Hiroki Honda‡, Tetsuya Sasaki‡, Hideki Yasukawa‡, Ryo Hayakawa§

* Kyoto University, Kyoto, Japan ╱ RIKEN Center for Advanced Intelligence Project
E-mail: hayashi.kazunori.4w@kyoto-u.ac.jp
† Kyoto University, Kyoto, Japan
E-mail: nakai.ayano@sys.i.kyoto-u.ac.jp
‡ Osaka City University, Osaka, Japan
E-mail: m20tb035@ka.osaka-cu.ac.jp, m20tb040@zy.osaka-cu.ac.jp,
m20tb018@zp.osaka-cu.ac.jp, m20tb047@hj.osaka-cu.ac.jp
§ Osaka University, Osaka, Japan
E-mail: rhayakawa@sys.es.osaka-u.ac.jp

Abstract—**This paper proposes a signal detection method for overloaded massive multi-user multi-input multi-output (MU-MIMO) orthogonal frequency division multiplexing (OFDM) and single carrier block transmission with cyclic prefix (SC-CP) systems by using sum of complex sparse regularizers (SCSR) as the regularizer of the discreteness of transmitted signal. Main feature of this work is that non-convex sparse regularizers are newly considered, while convex sparse regularizers only are considered in our previous work on the overloaded MIMO signal detection. Numerical results demonstrate that the proposed approach with the appropriate choice of the non-convex sparse regularizer can achieve better symbol error rate (SER) performance than that with the convex regularizer, and also that the precoding by Hadamard matrix or discrete Fourier transform (DFT) matrix is significantly beneficial for the case with non-convex sparse regularizers as well. Moreover, unlike the case with the ideal independent and identically distributed (i.i.d.)Gaussian measurement matrix, the regularizer based on $\ell_{2/3}$ norm or $\ell_{1/2}$ norm can achieve better SER performance than that with ℓ_0 norm based regularizer under the simulation condition.**

Index Terms—**Overloaded MIMO, Discreteness, Sparsity, IoT, Non-convex Regularizer**

I. INTRODUCTION

Typical use cases of the 5th generation mobile communications systems (5G) [1], [2] include the data collection from a large number of internet-of-things (IoT) nodes using a base station with a large number of antennas. The data collection problem can be modeled as a massive multi-user multi-input multi-output (MU-MIMO) communications system by regarding each IoT node as a transmit antenna, however, there is a fundamental difference between the conventional massive MU-MIMO [3], [4] and the IoT data collection environment that the number of transmit antennas (transmit streams) is typically greater than that of receiving antennas even when a

massive antenna array is employed at the base station, which results in what we call overloaded MIMO or underdetermined MIMO.

The signal detection problem of overloaded MIMO is very difficult due to the underdetermined nature of the problem. However, if we have some prior knowledge on the transmitted signal, it might be possible to uniquely determine the transmitted signal from its underdetermined linear measurements. Taking advantage of the fact that the transmitted symbol of digital communications takes discrete values on a finite set (i.e., alphabet), we can achieve overloaded MIMO signal detection based on maximum likelihood (ML) approach [5]. Moreover, since the ML approach is not tractable due to high computational complexity for massive overloaded MIMO signal detection, we have proposed a low complexity MIMO orthogonal frequency devision multiplexing (OFDM) signal detection scheme using convex optimization [10], where sum-of-absolute-values (SOAV) optimization [8], which is based on the idea of compressed sensing [6], [7], is employed. In [10], it has been shown that the proposed IoT signal detection can achieve almost the same performance as in the case with the independent and identically distributed (i.i.d.) Gaussian measurement matrix, which can be considered as an ideal case, by multiplying a common Hadamard matrix at IoT nodes (transmitters) as a precoding matrix. Furthermore, we have extended the method in [10] to the signal detection of overloaded MU-MIMO single carrier block transmission with cyclic prefix (SC-CP) in complex domain [11] in order to take the dependency between the real and the imaginary parts of the transmitted symbol into consideration by using sum of complex sparse regularizers (SCSR) optimization [12].

In this paper, we try to further improve the signal detection performance of SCSR approach for overloaded MU-MIMO OFDM and SC-CP systems by using non-convex sparse regularizers using our recent algorithm in [9] since we have considered convex sparse regularizers only in [10] and [11].

Numerical results demonstrate that the proposed approach with the appropriate choice of the non-convex sparse regularizer can achieve better symbol error rate (SER) performance than that with the convex regularizer, and also that the precoding by Hadamard matrix or discrete Fourier transform (DFT) matrix is significantly beneficial for the case with non-convex sparse regularizers as well. Moreover, unlike the case with the ideal Gaussian measurement matrix considered in [9], the regularizer based on $\ell_{2/3}$ norm or $\ell_{1/2}$ norm can achieve better SER performance than that with ℓ_0 norm based regularizer under the simulation condition.

In the rest of the paper, we use the following notations. $\mathbb{R}$ is the set of all real numbers and $\mathbb{C}$ is the set of all complex numbers. We represent the transpose by $(\cdot)^{\mathrm{T}}$, the Hermitian transpose by $(\cdot)^{\mathrm{H}}$, the imaginary unit by j, the $N \times N$ identity matrix by $\boldsymbol{I}_N$, a vector of size $N \times 1$ whose elements are all 1 by $\boldsymbol{1}_N$, and a vector of size $N \times 1$ whose elements are all 0 by $\boldsymbol{0}_N$. $\mathrm{Re}\{\cdot\}$ and $\mathrm{Im}\{\cdot\}$ denote the real part and the imaginary part, respectively. For $\boldsymbol{u} = [u_1 \cdots u_N]^{\mathrm{T}}$ and some operator f, $[f(\boldsymbol{u})]_n$ and u_n denote the n-th element of $f(\boldsymbol{u})$ and $\boldsymbol{u}$, respectively. For a lower semicontinuous function $\phi : \mathbb{K}^N \to \mathbb{R} \cup \{\infty\}$ ($\mathbb{K} = \mathbb{R}$ or $\mathbb{C}$), the proximity operator of $\phi(\cdot)$ is defined as $\mathrm{prox}_\phi(\boldsymbol{u}) = \arg\min_{\boldsymbol{s} \in \mathbb{K}^N} \left\{ \phi(\boldsymbol{s}) + \frac{1}{2}\|\boldsymbol{s} - \boldsymbol{u}\|_2^2 \right\}$.

II. SYSTEM MODEL

Here, we introduce the system model considered in this paper. Fig. 1 shows the transmitter/receiver structure of the uplink IoT signal collection environment, which is modelled by the overloaded MU-MIMO with precoded OFDM signaling. The number of IoT nodes is assumed to be N, the number of subcarriers to be Q and $\boldsymbol{s}_n \in \mathbb{C}^Q$ ($n = 1, \ldots, N$) is the transmitted signal block (OFDM symbol) in the frequency domain from the n-th IoT node, which is transmitted after the precoding by a matrix $\boldsymbol{P} \in \mathbb{C}^{Q \times Q}$, inverse discrete Fourier transform (IDFT) and the addition of cyclic prefix (CP). Then, the frequency domain received signal model of the precoded MU-MIMO OFDM can be written as

$$
\begin{bmatrix} \boldsymbol{r}_1^{\mathrm{ofdm}} \\ \vdots \\ \boldsymbol{r}_M^{\mathrm{ofdm}} \end{bmatrix}
$$
$$
= \begin{bmatrix} \boldsymbol{\Lambda}_{1,1}\boldsymbol{D} & \cdots & \boldsymbol{\Lambda}_{1,N}\boldsymbol{D} \\ \vdots & & \vdots \\ \boldsymbol{\Lambda}_{M,1}\boldsymbol{D} & \cdots & \boldsymbol{\Lambda}_{M,N}\boldsymbol{D} \end{bmatrix} \begin{bmatrix} \boldsymbol{D}^{\mathrm{H}}\boldsymbol{P}\boldsymbol{s}_1 \\ \vdots \\ \boldsymbol{D}^{\mathrm{H}}\boldsymbol{P}\boldsymbol{s}_N \end{bmatrix} + \begin{bmatrix} \boldsymbol{v}_1 \\ \vdots \\ \boldsymbol{v}_M \end{bmatrix},
$$
$$
= \begin{bmatrix} \boldsymbol{\Lambda}_{1,1}\boldsymbol{P} & \cdots & \boldsymbol{\Lambda}_{1,N}\boldsymbol{P} \\ \vdots & & \vdots \\ \boldsymbol{\Lambda}_{M,1}\boldsymbol{P} & \cdots & \boldsymbol{\Lambda}_{M,N}\boldsymbol{P} \end{bmatrix} \begin{bmatrix} \boldsymbol{s}_1 \\ \vdots \\ \boldsymbol{s}_N \end{bmatrix} + \begin{bmatrix} \boldsymbol{v}_1 \\ \vdots \\ \boldsymbol{v}_M \end{bmatrix}, \quad (1)
$$

where $\boldsymbol{r}_m^{\mathrm{ofdm}} \in \mathbb{C}^Q$ ($m = 1, \ldots, M$) is the frequency domain received signal block at the m-th antenna at the base

station, and $\boldsymbol{D}$ is a Q-point Unitary DFT matrix defined as

$$
\boldsymbol{D} = \frac{1}{\sqrt{Q}} \begin{bmatrix} 1 & 1 & \cdots & 1 \\ 1 & e^{-j\frac{2\pi \times 1 \times 1}{Q}} & \cdots & e^{-j\frac{2\pi \times 1 \times (Q-1)}{Q}} \\ \vdots & \vdots & & \vdots \\ 1 & e^{-j\frac{2\pi \times (Q-1) \times 1}{Q}} & \cdots & e^{-j\frac{2\pi \times (Q-1) \times (Q-1)}{Q}} \end{bmatrix}.
$$

The frequency domain diagonal channel matrix $\boldsymbol{\Lambda}_{m,n} \in \mathbb{C}^{Q \times Q}$ between the n-th IoT node and the m-th receiving antenna can be defined by using the channel impulse response $\{h_1^{(m,n)}, \ldots, h_L^{(m,n)}\}$ with the order of $L - 1$ as

$$
\begin{bmatrix} \lambda_1^{(m,n)} \\ \vdots \\ \lambda_Q^{(m,n)} \end{bmatrix} = \sqrt{Q}\boldsymbol{D} \begin{bmatrix} h_1^{(m,n)} \\ \vdots \\ h_L^{(m,n)} \\ \boldsymbol{0}_{Q-L} \end{bmatrix}, \quad (2)
$$

where $\{\lambda_1^{(m,n)}, \ldots, \lambda_Q^{(m,n)}\}$ are diagonal elements of $\boldsymbol{\Lambda}_{m,n}$.

Note that the additive noise $\boldsymbol{v}_m \in \mathbb{C}^Q$ at the m-th receiving antenna having mean $\boldsymbol{0}_Q$ and covariance matrix $\sigma_v^2 \boldsymbol{I}_Q$ will be added before the removal of the CP in practice, but taking advantage of the mathematical equivalence of the noise in time and frequency domains due to the property of Unitary matrix $\boldsymbol{D}$, we have employed the model shown in Fig. 1.

$\boldsymbol{P}$ is a precoding matrix required to achieve good detection performance in the case of the convex optimization based detection scheme in our previous work [10], [11], where we have numerically confirmed that a common Hadamard matrix or a common DFT matrix can lead to good SER performance. In the case of non-convex optimization based approach, we are not sure whether the precoding matrix is necessary or not, and thus we'll examine the detection performance for the cases with and without the precoding in Sect. V.

If we employ the DFT matrix $\boldsymbol{D}$ for the precoding matrix $\boldsymbol{P}$, the signal model results in the overloaded MU-MIMO SC-CP signaling as we have shown in [11]. Specifically, by setting $\boldsymbol{P} = \boldsymbol{D}$ in (1) and using the fact of $\boldsymbol{D}^{\mathrm{H}}\boldsymbol{D} = \boldsymbol{I}_Q$, we have

$$
\begin{bmatrix} \boldsymbol{r}_1^{\mathrm{sccp}} \\ \vdots \\ \boldsymbol{r}_M^{\mathrm{sccp}} \end{bmatrix} = \begin{bmatrix} \boldsymbol{\Lambda}_{1,1}\boldsymbol{D} & \cdots & \boldsymbol{\Lambda}_{1,N}\boldsymbol{D} \\ \vdots & & \vdots \\ \boldsymbol{\Lambda}_{M,1}\boldsymbol{D} & \cdots & \boldsymbol{\Lambda}_{M,N}\boldsymbol{D} \end{bmatrix} \begin{bmatrix} \boldsymbol{s}_1 \\ \vdots \\ \boldsymbol{s}_N \end{bmatrix} + \begin{bmatrix} \boldsymbol{v}_1 \\ \vdots \\ \boldsymbol{v}_M \end{bmatrix},
$$
$$
\tag{3}
$$

which can be easily verified to be the received signal model of the SC-CP signaling in the discrete frequency domain by multiplying a unitary matrix of

$$
\begin{bmatrix} \boldsymbol{D} & 0 & \cdots & 0 \\ 0 & \boldsymbol{D} & & \vdots \\ \vdots & & \ddots & 0 \\ 0 & \cdots & \cdots & \boldsymbol{D} \end{bmatrix}^{\mathrm{H}} \in \mathbb{C}^{QM \times QM} \quad (4)
$$

from the left of both sides. Thus, the MU-MIMO SC-CP signaling without precoding can be regarded as a special case of the MU-MIMO OFDM signaling with precoding. Fig. 2 shows the transmitter/receiver structure of the uplink
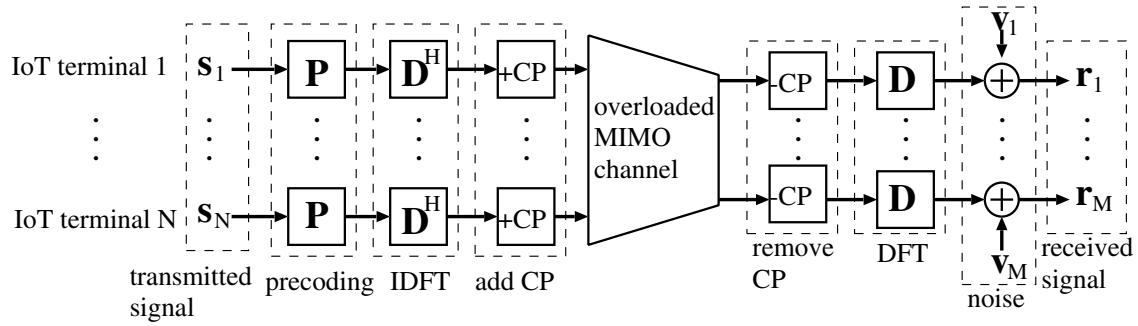
Fig. 1. Transmitter/Receiver structure of precoded OFDM
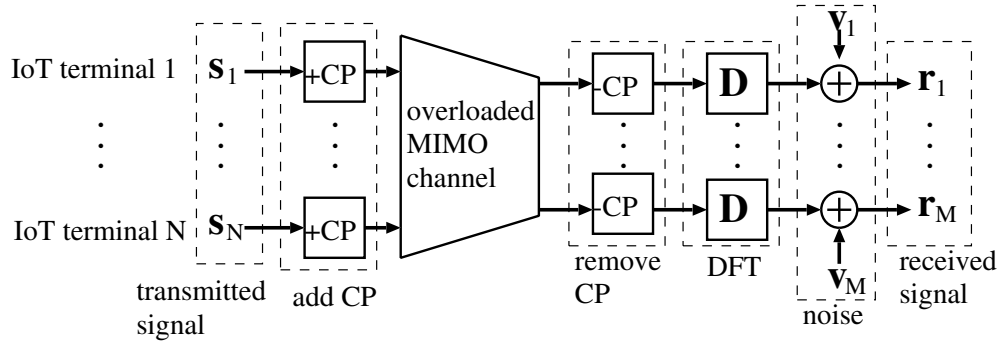
Fig. 2. Transmitter/Receiver structure of non-precoded SC-CP

IoT signal collection environment, which is model by the overloaded MU-MIMO with non-precoded SC-CP signaling. If DFT matrix $\boldsymbol{D}$ is appropriate for the precoding matrix of overloaded MU-MIMO OFDM system with the non-convex optimization based signal detection as well, then the choice of SC-CP signaling is highly suited for IoT environments because it requires neither the IDFT operation nor the precoding operation at the IoT node.

III. COMPLEX DISCRETE VALUED SIGNAL RECONSTRUCTION VIA SCSR OPTIMIZATION WITH NON-CONVEX SPARSE REGULARIZERS

One of features of the proposed approach in this paper is the employment of non-convex sparse regularizers in SCSR optimization, instead of convex sparse regularizers as in [10] or [11]. Here, we briefly review the complex discrete-valued vector reconstruction by SCSR optimization with non-convex sparse regularizers [9].

We consider the reconstruction problem of a complex discrete-valued vector $\boldsymbol{x} = [x_1 \cdots x_N]^{\mathrm{H}} \in \mathcal{C}^N \subset \mathbb{C}^N$ from a linear measurement given by

$$\boldsymbol{y} = \boldsymbol{A}\boldsymbol{x} + \boldsymbol{n} \in \mathbb{C}^M, \qquad (5)$$

where we assume $M < N$. Here, $\mathcal{C} = \{c_1 \cdots c_S\}$ is a set of discrete values, that each element of unknown vector $\boldsymbol{x}$ takes, and the probability distribution of each element of $\boldsymbol{x}$ is given

by

$$\Pr(x_n = c_\ell) = p_\ell, \ (\ell = 1, \ldots, S), \qquad (6)$$

where $\sum_{\ell=1}^S p_\ell = 1$. $\boldsymbol{A} \in \mathbb{C}^{M \times N}$ is a linear measurement matrix and $\boldsymbol{n} \in \mathbb{C}^M$ is an additive noise vector with mean of $\boldsymbol{0}_M$ and covariance matrix of $\sigma_n^2 \boldsymbol{I}_M$.

The optimization problem for the complex discrete-valued signal reconstruction with SCSR is given by

$$\underset{\boldsymbol{x} \in \mathbb{C}^N}{\text{minimize}} \ \left\{ \sum_{\ell=1}^S q_\ell g_\ell(\boldsymbol{x} - c_\ell \boldsymbol{1}) + \lambda \|\boldsymbol{y} - \boldsymbol{A}\boldsymbol{x}\|_2^2 \right\}, \quad (7)$$

where $\lambda \geq 0$ and $\sum_{\ell=1}^S q_\ell = 1 \ (q_l \geq 0)$ are parameters. The function $g_\ell(\cdot)$ is a non-convex sparse regularizer, but we assume that its proximity operator can be computed efficiently in this paper. Here, it should be noted that the proximity operator for the case of non-convex sparse regularizer is nothing but a formal one, because the proximity operator is defined only for convex functions. Also, please note that the sum of sparse regularizers in (7) forms a regularizer to promote the discreteness of each element of unknown vector $\boldsymbol{x}$.

If we employ a convex sparse regularizer for $g_\ell(\cdot)$, such as

$$g_\star^{(1)}(\boldsymbol{u}) = \|\boldsymbol{u}\|_1 = \sum_{n=1}^{N} \sqrt{\mathrm{Re}\{u_n\}^2 + \mathrm{Im}\{u_n\}^2}, \quad (8)$$

$$g_{\star\star}^{(1)}(\boldsymbol{u}) = \|\mathrm{Re}\{\boldsymbol{u}\}\|_1 + \|\mathrm{Im}\{\boldsymbol{u}\}\|_1 \quad (9)$$

$$= \sum_{n=1}^{N}(|\mathrm{Re}\{u_n\}| + |\mathrm{Im}\{u_n\}|), \quad (10)$$

where $\boldsymbol{u} = [u_1 \cdots u_N]^{\mathrm{T}} \in \mathbb{C}^N$, then the detection method by SCSR optimization results in method proposed in [11]. The proximity operators of $\gamma g_\star^{(1)}(\cdot)$ and $\gamma g_{\star\star}^{(1)}(\cdot)$ ($\gamma > 0$) are respectively given by

$$[\mathrm{prox}_{\gamma g_\star^{(1)}(\cdot)}(\boldsymbol{u})]_n = \begin{cases} (|u_n| - \gamma)\frac{u_n}{|u_n|} & (|u_n| \geq \gamma) \\ 0 & (|u_n| < \gamma), \end{cases}$$

and

$$[\mathrm{prox}_{\gamma g_{\star\star}^{(1)}}(\boldsymbol{u})]_n = \mathrm{sign}([\mathrm{Re}(\boldsymbol{u})]_n)\max(|[\mathrm{Re}(\boldsymbol{u})]_n| - \gamma, 0)$$
$$+ j \cdot \mathrm{sign}([\mathrm{Im}(\boldsymbol{u})]_n)\max(|[\mathrm{Im}(\boldsymbol{u})]_n| - \gamma, 0).$$

As examples of non-convex sparse regularizers, we can consider the regularizer based on ℓ_p $(0 < p < 1)$ norm as

$$g_\star^{(p)}(\boldsymbol{u}) = \sum_{n=1}^{N} |u_n|^p \quad (11)$$

and

$$g_{\star\star}^{(p)}(\boldsymbol{u}) = \sum_{n=1}^{N}(|\mathrm{Re}\{u_n\}|^p + |\mathrm{Im}\{u_n\}|^p), \quad (12)$$

where the former $g_\star^{(p)}(\cdot)$ is based on the modulus for complex numbers, whereas the latter $g_{\star\star}^{(p)}(\cdot)$ treats the real part and the imaginary part independently. The proximity operator of $\gamma g_\star^{(p)}(\cdot)$ can be obtained from the proximity operator of the corresponding regularizer $g^{(p)}(\cdot)$ in the real domain (i.e., $g^{(p)}(\boldsymbol{q}) = \|\boldsymbol{q}\|_p^p = \sum_{n=1}^{N} |q_n|^p$ for $\boldsymbol{q} = [q_1 \cdots q_N]^{\mathrm{T}} \in \mathbb{R}^N$). By using the relation $g_\star^{(p)}(\boldsymbol{u}) = g^{(p)}(|\boldsymbol{u}|)$, where $|\boldsymbol{u}| = [|u_1| \cdots |u_N|]^{\mathrm{T}}$, the proximity operator of $\gamma g_\star^{(p)}(\cdot)$ can be derived from that of $\gamma g^{(p)}(\cdot)$ as

$$[\mathrm{prox}_{\gamma g_\star^{(p)}}(\boldsymbol{u})]_n = [\mathrm{prox}_{\gamma g^{(p)}}(|\boldsymbol{u}|)]_n \frac{u_n}{|u_n|} \quad (13)$$

with a simple manipulation. The proximity operator of $\gamma g_{\star\star}^{(p)}(\cdot)$ also can be written with the corresponding proximity operator $\mathrm{prox}_{\gamma g^{(p)}}(\cdot)$. Since we have $g_{\star\star}^{(p)}(\boldsymbol{u}) = g^{(p)}(\mathrm{Re}\{\boldsymbol{u}\}) + g^{(p)}(\mathrm{Im}\{\boldsymbol{u}\})$ from the definition, the proximity operator can be written as

$$[\mathrm{prox}_{\gamma g_{\star\star}^{(p)}}(\boldsymbol{u})]_n = [\mathrm{prox}_{\gamma g^{(p)}}(\mathrm{Re}\{\boldsymbol{u}\})]_n$$
$$+ j \cdot [\mathrm{prox}_{\gamma g^{(p)}}(\mathrm{Im}\{\boldsymbol{u}\})]_n \quad (14)$$

by using a similar approach to [12]. The proximity operator of the ℓ_p norm based regularizers in the real domain has been discussed in [16], [17], [18]. For arbitrary $p \in (0, 1)$, we can

---

Algorithm 1 ADMM-SNSR

Require: $\boldsymbol{y} \in \mathbb{C}^M, \boldsymbol{A} \in \mathbb{C}^{M \times N}$
Ensure: $\boldsymbol{x} \in \mathbb{C}^N$
 1: Fix $\rho > 0$, $\boldsymbol{z}^0 \in \mathbb{C}^{SN}$, $\boldsymbol{w}^0 \in \mathbb{C}^{SN}$
 2: **for** $k = 0$ to $K - 1$ **do**
 3:     $\boldsymbol{x}^{k+1} = (\rho S \boldsymbol{I}_N + \lambda \boldsymbol{A}^{\mathrm{H}} \boldsymbol{A})^{-1}(\rho \sum_{\ell=1}^{S}(\boldsymbol{z}_\ell^k - \boldsymbol{w}_\ell^k) + \lambda \boldsymbol{A}^{\mathrm{H}} \boldsymbol{y})$
 4:     $\boldsymbol{z}_\ell^{k+1} = c_\ell \mathbf{1} + \mathrm{prox}_{\frac{q_\ell}{2\rho} g_\ell}(\boldsymbol{x}^{k+1} + \boldsymbol{w}_\ell^k - c_\ell \mathbf{1})$ $(\ell = 1, \ldots, S)$
 5:     $\boldsymbol{w}_\ell^{k+1} = \boldsymbol{w}_\ell^k + \boldsymbol{x}^{k+1} - \boldsymbol{z}_\ell^{k+1}$ $(\ell = 1, \ldots, S)$
 6: **end for**
 7: $\boldsymbol{x} = \mathcal{Q}(\boldsymbol{x}^K)$

---

numerically compute the proximity operator, while the proximity operator for specific values of p such as $p = 1/2, 2/3$ can be written explicitly.

Another non-convex regularizer $g_\star^{(0)}(\cdot)$ or $g_{\star\star}^{(0)}(\cdot)$ can be obtained with the similar approach as $g_\star^{(p)}(\cdot)$ or $g_{\star\star}^{(p)}(\cdot)$ from the ℓ_0 norm based regularizer $g^{(0)}(\mathrm{Re}\{\boldsymbol{u}\}) = \|\mathrm{Re}\{\boldsymbol{u}\}\|_0$ in real domain. Specifically, the proximity operator of $\gamma g^{(0)}(\cdot)$ is given by $[\mathrm{prox}_{\gamma g^{(0)}}(\boldsymbol{u})]_n = 0$ when $|u_n| < \sqrt{2\gamma}$, $[\mathrm{prox}_{\gamma g^{(0)}}(\boldsymbol{u})]_n = \{0, u_n\}$ when $|u_n| = \sqrt{2\gamma}$, and $[\mathrm{prox}_{\gamma g^{(0)}}(\boldsymbol{u})]_n = u_n$ when $|u_n| > \sqrt{2\gamma}$ $(n = 1, \ldots, N)$, and the proximity operator of $\gamma g_\star^{(0)}(\cdot)$ and $\gamma g_{\star\star}^{(0)}(\cdot)$ can be obtained by using (13) and (14), respectively.

Yet another example of non-convex regularizer will be $g_\star^{(1-2)}(\cdot)$ or $g_{\star\star}^{(1-2)}(\cdot)$, whose corresponding regularizer in real domain is the $\ell_1 - \ell_2$ difference given by $g^{(1-2)}(\boldsymbol{u}) = \|\boldsymbol{u}\|_1 - \|\boldsymbol{u}\|_2$ originally proposed for compressed sensing [19], [20]. The proximity operator of $g^{(1-2)}(\cdot)$ can be computed with Lemma 1 in [20] or Proposition 7.1 in [21].

The ADMM based algorithm to solve SCSR optimization problem (7) is summarized in Algorithm 1, where $\mathcal{Q}(\cdot)$ denotes the element-wise quantization operator which maps the input to its nearest value in $\mathbb{C}$. As we can see from the algorithm, we can obtain the estimate of the unknown vector $\boldsymbol{x}$ as far as the proximity operator of the sparse regularizer involved in the optimization is available, however, in the case of non-convex sparse regularizer, the estimate obtained by the ADMM based algorithm might not be the global optimizer of (7).

IV. OVERLOADED IoT SIGNAL DETECTION VIA SNSR OPTIMIZATION

Both received signal models of the precoded MU-MIMO OFDM signaling (1) and the non-precoded MU-MIMO SC-CP signaling (3) can be given by the form

$$\boldsymbol{r} = \boldsymbol{H}\boldsymbol{s} + \boldsymbol{v}, \quad (15)$$

where $\boldsymbol{r} \in \mathbb{C}^{QM}$ is a received signal vector, $\boldsymbol{s} \in \mathbb{C}^{QN}$ is a transmitted signal vector, $\boldsymbol{H} \in \mathbb{C}^{QM \times QN}$ is a channel matrix,

and $\boldsymbol{v} \in \mathbb{C}^{QM}$ is a white additive noise vector, by regarding

$$\boldsymbol{r} = \begin{bmatrix} \boldsymbol{r}_1^{\mathrm{ofdm}} \\ \vdots \\ \boldsymbol{r}_M^{\mathrm{ofdm}} \end{bmatrix}, \quad \boldsymbol{s} = \begin{bmatrix} \boldsymbol{s}_1 \\ \vdots \\ \boldsymbol{s}_N \end{bmatrix}, \quad \boldsymbol{v} = \begin{bmatrix} \boldsymbol{v}_1 \\ \vdots \\ \boldsymbol{v}_M \end{bmatrix},$$

$$\boldsymbol{H} = \begin{bmatrix} \boldsymbol{\Lambda}_{1,1}\boldsymbol{P} & \cdots & \boldsymbol{\Lambda}_{1,N}\boldsymbol{P} \\ \vdots & & \vdots \\ \boldsymbol{\Lambda}_{M,1}\boldsymbol{P} & \cdots & \boldsymbol{\Lambda}_{M,N}\boldsymbol{P} \end{bmatrix},$$

for the case with the precoded MU-MIMO OFDM signaling, and

$$\boldsymbol{r} = \begin{bmatrix} \boldsymbol{r}_1^{\mathrm{sccp}} \\ \vdots \\ \boldsymbol{r}_M^{\mathrm{sccp}} \end{bmatrix}, \quad \boldsymbol{s} = \begin{bmatrix} \boldsymbol{s}_1 \\ \vdots \\ \boldsymbol{s}_N \end{bmatrix}, \quad \boldsymbol{v} = \begin{bmatrix} \boldsymbol{v}_1 \\ \vdots \\ \boldsymbol{v}_M \end{bmatrix},$$

$$\boldsymbol{H} = \begin{bmatrix} \boldsymbol{\Lambda}_{1,1}\boldsymbol{D} & \cdots & \boldsymbol{\Lambda}_{1,N}\boldsymbol{D} \\ \vdots & & \vdots \\ \boldsymbol{\Lambda}_{M,1}\boldsymbol{D} & \cdots & \boldsymbol{\Lambda}_{M,N}\boldsymbol{D} \end{bmatrix},$$

for the case with the non-precoded MU-MIMO SC-CP signaling.

The SCSR optimization problem for (15) is given by

$$\underset{\boldsymbol{x} \in \mathbb{C}^N}{\mathrm{minimize}} \left\{ \sum_{\ell=1}^{S} q_\ell g_\ell(\boldsymbol{s} - c_\ell \boldsymbol{1}) + \lambda \|\boldsymbol{r} - \boldsymbol{H}\boldsymbol{s}\|_2^2 \right\}, \quad (16)$$

where we have $S = 4$, $(c_1, c_2, c_3, c_4) = \{1 + j, -1 + j, 1 - j, -1 - j\}$, if we assume QPSK modulation. Note that, if transmit symbol does not include non-active IoT nodes (i.e. symbol of 0), the sparse regularizers of $g_\star^{(0)}(\cdot)$, $g_\star^{(1)}(\cdot)$, $g_\star^{(p)}(\cdot)$, $g_\star^{(1-2)}(\cdot)$ will be appropriate for $g_\ell(\cdot)$, however, if we have some non-active nodes, the employment of the sparse regularizers of $g_{\star\star}^{(0)}(\cdot)$, $g_{\star\star}^{(1)}(\cdot)$, $g_{\star\star}^{(p)}(\cdot)$, $g_{\star\star}^{(1-2)}(\cdot)$ could be beneficial because it can utilize the fact that the real and the imaginary parts of the non-active node take the value of 0 simultaneously.

V. NUMERICAL RESULTS

We have conducted numerical experiments via computer simulations to evaluate the SER performance of the proposed overloaded signal detection scheme for the MU-MIMO OFDM signaling and the MU-MIMO SC-CP signaling in multi-path Rayleigh fading channels. The block size of OFDM and SC-CP transmission is set to $Q = 64$, and the length of the cyclic prefix is assumed to be greater than or equal to the channel order $L - 1 = 9$. In order to evaluate the performance of different system size, we have set the number of antennas at the base station M and the number of IoT nodes N to be $(M, N) = (4, 5)$ and $(M, N) = (40, 50)$, which correspond to the overloaded factor of 1.25 for both sizes. In order to verify the impact of the precoding, we evaluate the performance of the overloaded MU-MIMO OFDM signaling with and without precoding, while we consider non-precoded case only for the overloaded MU-MIMO SC-CP signaling since the precoding is embedded inherently. Since we do not consider the existence of non-active nodes in this simulation,

we evaluate the performance with the sparse regularizers of $g_\star^{(1)}(\cdot)$, $g_\star^{2/3)}(\cdot)$, $g_\star^{(1/2)}(\cdot)$, $g_\star^{(0)}(\cdot)$, and $g_\star^{(1-2)}(\cdot)$, which are denoted as ℓ_1, $\ell_{2/3}$, $\ell_{1/2}$, ℓ_0, and $\ell_1 - \ell_2$, respectively in the following figures. Note that the employment of $g_\star^{(1)}(\cdot)$ (and hence ℓ_1) is equivalent to the method in [11].

Figs. 3 and 4 show the SER performance of MU-MIMO OFDM without precoding with the system sizes of $M = 4$, $N = 5$ and $M = 40$, $N = 50$, respectively. From the figures, we can see that small size MU-MIMO OFDM system without precoding suffers from poor SER performance for all sparse regularizers, while the performance is significantly improved for the large system. It should be noted that, although some non-convex sparse regularizers can outperform the convex sparse regularizer (ℓ_1) in Fig. 4, other non-convex sparse regularizers achieve worse performance than that of the convex sparse regularizer. Thus, appropriate choice of non-convex sparse regularizer will be important for the non-precoded MU-MIMO OFDM signaling with large size. It is also interesting to see that ℓ_0 regularizer, which has achieved the best performance for the case with the ideal i.i.d. Gaussian measurement matrix in [9], has the worst performance for the detection of non-precoded MU-MIMO OFDM signal with large size.

Figs. 5 and 6 show the SER performance of MU-MIMO OFDM with precoding by Hadamard matrix with the system sizes of $M = 4$, $N = 5$ and $M = 40$, $N = 50$, respectively. We can see that the performance is significantly improved compared as that in Figs. 3 and 4, which implies that the precoding by Hadamard matrix is quite beneficial for the proposed overloaded MU-MIMO OFDM detection with non-convex sparse regularizers as well. Moreover, all non-convex sparse regularizers except for $\ell_1 - \ell_2$ achieve better performance than that of the convex sparse regularizer (ℓ_1), which demonstrates the validity of the proposed approach in this paper.

Figs. 7 and 8 show the SER performance of MU-MIMO SC-CP without precoding with the system sizes of $M = 4$, $N = 5$ and $M = 40$, $N = 50$, respectively. The performance of all sparse regularizers in Figs. 7 and 8 is almost equivalent to that in Figs. 5 and 6, which demonstrates the suitability of SC-CP for IoT environment, which has claimed in our previous work in [9], still holds for the case of the SCSR with non-convex sparse regularizers. From all the numerical results, the non-convex sparse regularizer of $\ell_{2/3}$ or $\ell_{1/2}$ could be the best choice for this specific simulation setting.

VI. CONCLUSION

We have considered the overloaded signal detection problem for uplink IoT environments and have proposed SCSR optimization approach with non-convex sparse regularizers for the overloaded MU-MIMO OFDM and SC-CP signaling. The validity of the proposed approach using precoded OFDM signaling or non-precoded SC-CP signaling has been confirmed via computer experiments. One of important findings in this paper will be that the choice of $\ell_{2/3}$ or $\ell_{1/2}$ could be better than ℓ_0 in the signal detection problem, while ℓ_0 has achieved
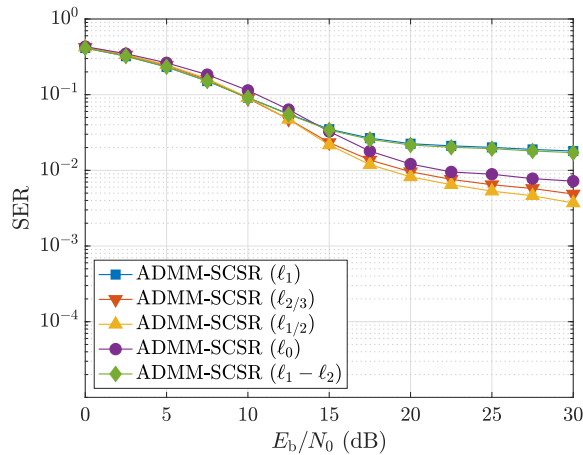
Fig. 3. SER performance (OFDM without precoding, $M = 4$, $N = 5$)
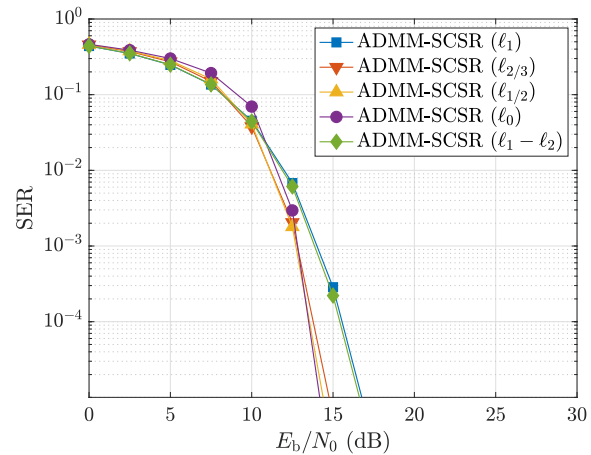
Fig. 5. SER performance (OFDM with precoding, $M = 4$, $N = 5$)
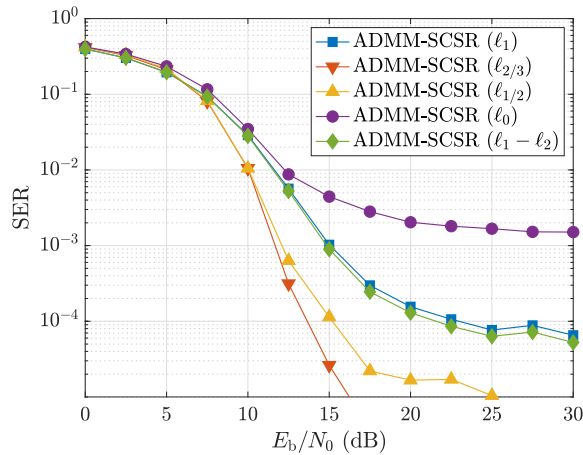
Fig. 4. SER performance (OFDM without precoding, $M = 40$, $N = 50$)
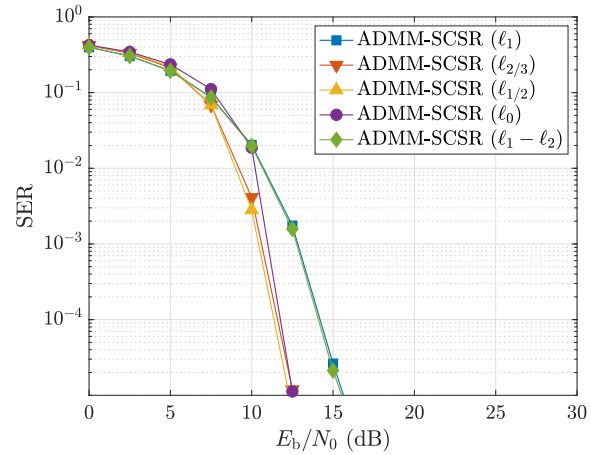
Fig. 6. SER performance (OFDM with precoding, $M = 40$, $N = 50$)

better performance than $\ell_{2/3}$ and $\ell_{1/2}$ for the case of very large i.i.d. Gaussian linear measurement matrix in [9].

Future work includes the investigations of the performance for the case with non-active IoT nodes and also taking advantage of group sparsity in the block transmission schemes. Furthermore, the impact of channel coding should be evaluated because it may have some impact on the error floor observed in the simulations of OFDM without precoding.

REFERENCES

[1] A. Gupta and R. K. Jha, "A survey of 5G network: Architecture and emerging technologies," *IEEE Access*, vol. 3, pp. 1206–1232, July 2015.

[2] J. G. Andrews, S. Buzzi, W. Choi, S. V. Hanly, A. Lozano, A. C. Soong, and J. C. Zhang, "What will 5G be?," *IEEE Journal on Selected Areas in Communications*, vol. 32, no. 6, pp. 1065–1082, June 2014.

[3] A. K. Saxena, I. Fijalkow, A. L. Swindlehurst, "Analysis of one-bit quantized precoding for the multiuser massive MIMO downlink," *IEEE Trans. on Signal Process.*, vol. 65, no. 17, pp.4624–4634, Sep. 2017.

[4] S. Jacobsson, G. Durisi, M. Coldrey, C. Studer, "Massive MU-MIMO-OFDM downlink with one-bit DACs and linear precoding," 2017.

[Online]. Available: http://arxiv.org/abs/1704.04607

[5] Y. Nin, H. Matsuoka, Y. Sanada, "Performance comparison of overloaded MIMO system with and without antenna selection," *IEICE Trans. Commun.,* vol. E100-B, no. 5, pp. 762–770, May 2017.

[6] D. L. Donoho, "Compressed sensing," *IEEE Trans. Inf. Theory*, vol. 52, no. 4, pp. 1289–1306, Apr. 2006.

[7] K. Hayashi, M. Nagahara, T. Tanaka "A user's guide to compressed sensing for communications systems," *IEICE Trans. Commun.,* vol. E96-B, no. 3, pp. 685–712, Mar. 2013.

[8] R. Hayakawa, K. Hayashi, "Convex optimization-based signal detection for massive overloaded MIMO systems," *IEEE Trans. Wireless Commun.,* vol. 16, no. 11, pp. 7080–7091, Nov. 2017.

[9] R. Hayakawa and K. Hayashi, "Discrete-Valued Vector Reconstruction by Optimization with Sum of Sparse Regularizers", *in Proc. European Signal Processing Conference (EUSIPCO2019),* A Coruna, Spain, pp. 1-5, Sept. 2019.

[10] K. Hayashi, A. Nakai, R. Hayakawa, S. Ha, "Uplink Overloaded MU-MIMO OFDM Signal Detection Methods using Convex Optimization", *in Proc. 2018 APSIPA Annual Summit and Conference (APSIPA ASC 2018),* Honolulu, Hawaii, USA, pp. 1421-1427, Nov. 2018.

[11] K. Hayashi, A. Nakai, R. Hayakawa, "An Overloaded SC-CP IoT Signal Detection Method via Sparse Complex Discrete-Valued Vector Reconstruction", *in Proc. 2019 APSIPA Annual Summit and Conference*
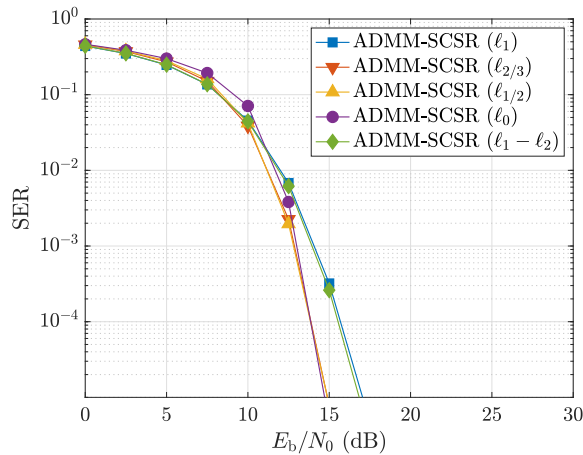
Fig. 7. SER performance (SC-CP without precoding, $M = 4$, $N = 5$)

Fig. 8. SER performance (SC-CP without precoding, $M = 40$, $N = 50$)

(APSIPA ASC 2019), Lanzhou, China, pp. 1473-1478, Nov. 2019.

[12] R. Hayakawa and K. Hayashi, "Reconstruction of complex discrete-valued vector via convex optimization with sparse regularizers," *IEEE Access*, vol. 6, pp. 66 499–66 512, Dec. 2018.

[13] A. Beck and M. Teboulle, "A fast iterative shrinkage-thresholding algorithm for linear inverse problems," *SIAM J. Imag. Sci.,* vol. 2, no. 1, pp. 183–202, Mar. 2009.

[14] D. L. Donoho, A. Maleki, and A. Montanari, "Message-passing algorithms for compressed sensing," *Proc. Nat. Acad. Sci.,* vol. 106, no. 45, pp. 18914–18919, Nov. 2009.

[15] R. Hayakawa and K. Hayashi, "Discreteness-aware approximate message passing for discrete-valued vector reconstruction," *IEEE Trans. Signal Process.,* vol. 66, no. 24, pp. 6443–6457, Dec. 2018.

[16] Z. Xu, X. Chang, F. Xu and H. Zhang, "$L_{1/2}$ regularization: A thresholding representation theory and a fast solver," *IEEE Trans. Neural Netw. Learn. Syst.,* vol. 23, no. 7, pp. 1013–1027, July 2012.

[17] Y. Zhang and W. Ye, "$L_{2/3}$ regularization: Convergence of iterative thresholding algorithm,," *J. Vis. Commun. Image Represent.,* vol. 33, pp. 350–357, Oct. 2015.

[18] F. Chen, L. Shen, and B. W. Suter, "Computing the proximity operator of the ℓ_p norm with $0 < p < 1$," *IET Signal Process.,* vol. 10, no. 5, pp. 557–565, June 2016.

[19] P. Yin, Y. Lou, Q. He, and J. Xin, "Minimization of $\ell_1 - \ell_2$ for compressed sensing," *SIAM J. Sci. Comput.,* vol. 37, no. 1, pp. A536–

A563, Feb. 2015.

[20] Y. Lou and M. Yan, "Fast L1-L2 minimization via a proximal operator," *J. Sci. Comput.,* vol. 74, no. 2, pp. 767–785, Feb. 2018.

[21] T. Liu and T. K. Pong, "Further properties of the forward-backward envelope with applications to difference-of-convex programming," *Comput. Optim. Appl.,* vol. 67, no. 3, pp. 489–520, July 2017.